Environ. Sci. Technol. **2007**, *41,* 4690−4697

Seasonal and Regional Variations of Primary and Secondary Organic Aerosols over the Continental United States: Semi-Empirical Estimates and Model Evaluation

SHAOCAI YU,*,†,‡ PRAKASH V. BHAVE,*,† ROBIN L. DENNIS,† AND ROHIT MATHUR†

Atmospheric Sciences Modeling Division, Air Resources Laboratory, National Oceanic and Atmospheric Administration, Research Triangle Park, North Carolina 27711

Seasonal and regional variations of primary (OC_{pri}) and secondary (OC_{sec}) organic carbon aerosols across the continental United States for the year 2001 were examined by a semi-empirical technique using observed OC and elemental carbon (EC) data from 142 routine monitoring sites in mostly rural locations across the country, coupled with the primary OC/EC ratios, obtained from a chemical transport model (i.e., Community Multiscale Air Quality (CMAQ) model). This application yields the first non-mechanistic estimates of the spatial and temporal variations in OC_{pri} and OC_{sec} over an entire year on a continental scale. There is significant seasonal and regional variability in the relative contributions of OC_{pri} and OC_{sec} to OC. Over the continental United States, the median OC_{sec} concentrations are 0.13, 0.36, 0.63, 0.44, and 0.42 μg C m^{-3} in winter (DJF), spring (MAM), summer (JJA), fall (SON), and annual, respectively, making 21, 44, 51, 42, and 43% contributions to OC, respectively. OC_{pri} exceeds OC_{sec} in all seasons except summer. Regional analysis shows that the southeastern region has the highest concentration of OC_{pri} (annual median = 1.35 μg C m^{-3}), whereas the central region has the highest concentration of OC_{sec} (annual median = 0.76 μg C m^{-3}). The mechanistic OC_{sec} estimates from the CMAQ model were compared against the independently derived semi-empirical OC_{sec} estimates. The results indicate that the mechanistic model reproduced the monthly medians of the semi-empirical OC_{sec} estimates well over the northeast, southeast, midwest, and central regions in all months except the summer months (June, July, and August), during which the modeled regional monthly medians were consistently lower than the semi-empirical estimates. This indicates that the CMAQ model is missing OC_{sec} formation pathways that are important in the summer.

1. Introduction

Organic carbon (OC) is a significant component of fine particulate matter ($PM_{2.5}$) mass at most locations in the United States (*1*). Organic carbon may be either directly emitted to the atmosphere (primary OC, OC_{pri}) or formed through atmospheric oxidation of reactive organic gases (ROG) and subsequent gas-to-particle conversion processes (secondary OC, OC_{sec}). Organic carbon is a complex mixture of hundreds of different compounds (*2*). Analytical techniques for quantifying OC_{pri} and OC_{sec} concentrations do not yet exist. Thus, indirect techniques have been developed to estimate OC_{pri} and OC_{sec}. These indirect techniques can be broadly categorized as empirical (solely measurement-based), mechanistic (based on a mechanistic air quality model), or semi-empirical (involving measurements together with an air quality model). Empirical techniques include the use of elemental carbon (EC) as a tracer for OC_{pri} (*3*−*5*) and the use of particle-phase organic compounds as tracers for OC_{pri} (*6*−*8*). Of these, the EC-tracer technique has been applied most widely because EC measurements are readily available. A major difficulty in applying this method is that one must know the ambient ratio of primary OC to EC, $(OC/EC)_{pri}$, which is influenced by meteorological conditions and fluctuations in emissions (*3*). Large uncertainties in the speciation of PM emissions and the OC and EC measurements also add to the uncertainties affecting this method.

Mechanistic air quality models are an important means to estimate OC_{pri} and OC_{sec} concentrations with a high degree of coverage across space and time and are our only means to predict the response of OC_{pri} and OC_{sec} to future emission controls and/or climate changes. Currently, a large uncertainty exists with the mechanistic approach because of uncertainties in the ROG emissions, the chemical reaction kinetics of ROGs, and thermodynamic partitioning of the semivolatile ROG oxidation products between the gas and particle phases. Data are not available to directly evaluate mechanistic OC_{pri} and OC_{sec} estimates. To address the shortcomings of both the empirical and mechanistic approaches, Yu et al. (*9*) developed a new approach, called the "emission/transport of primary OC/EC ratio method." For brevity, we have renamed this approach the "semi-empirical EC-tracer technique." This technique combines the empirical EC-tracer method with a transport/emission model of OC_{pri} and EC to estimate the concentrations of OC_{sec} and OC_{pri}. The advantages of this method are that it can provide $(OC/EC)_{pri}$ ratios at any time and any place, and therefore, OC_{pri} and OC_{sec} concentrations can be estimated at any time and location where EC and OC measurements are available. Yu et al. (*9*) have applied this method successfully to estimate OC_{pri} and OC_{sec} across the United States from June 15 to August 31, 1999.

The purposes of this paper are 3-fold. First, we identify the locations where the semi-empirical EC-tracer approach should be exercised with caution due to low reliability of the $(OC/EC)_{pri}$ ratios. Second, we apply the semi-empirical technique to estimate OC_{pri} and OC_{sec} using a full year of data spanning the continental United States. Third, we compare the mechanistically modeled OC_{sec} estimates against the independently derived semi-empirical OC_{sec} estimates. This comparison helps identify shortcomings in our current understanding of OC_{sec} formation processes.

2. Methodology

2.1 Semi-Empirical EC-Tracer Technique. The semi-empirical EC-tracer technique employed in the present study follows the methodology of Yu et al. (*9*). Briefly, OC_{pri} and

* Address correspondence to either author. Phone: 919-541-0362 (S.Y.), 919-541-2194 (P.B.); fax: 919-541-1379 (S.Y. and P.B.); e-mail: yu.shaocai@epa.gov (S.Y.), bhave.prakash@epa.gov (P.B.).

† On assignment to National Exposure Research Laboratory, U.S. Environmental Protection Agency, Research Triangle Park, NC 27711.

‡ On assignment from Science and Technology Corporation, 10 Basil Sawyer Drive, Hampton, VA 23666-1393.

10.1021/es061535g CCC: $37.00
Published on Web 05/26/2007

OC_{sec} are estimated as

$$OC_{pri} = \min(OC_{tot}, (OC/EC)_{pri} \times EC) \quad (1)$$

$$OC_{sec} = OC_{tot} - OC_{pri} \quad (2)$$

where OC_{tot} is the measured OC concentration, EC is the measured EC concentration, and $(OC/EC)_{pri}$ is the primary OC-to-EC ratio calculated using an air quality model. In contrast to the approach of Yu et al. (*9*), OC_{pri} is constrained explicitly in eq 1 such that it may not exceed the total OC concentration. As a result, OC_{sec} is set to zero in cases where $(OC/EC)_{pri} > (OC_{tot}/EC)$. These cases are indicative of model overestimations of $(OC/EC)_{pri}$ and will be discussed below.

2.2 CMAQ Model Description. The values of $(OC/EC)_{pri}$ needed in eq 1 are obtained from the Community Multiscale Air Quality (CMAQ) model version 4.4 (http://www.cmaq-model.org/).The simulation period covers the 2001 calendar year with hourly resolution, and the modeling domain spans the continental United States with 36-km horizontal grids and 14 vertical layers. In the present study, hourly model results from the lowest vertical layer at the cells containing the monitoring sites are time-integrated to match the 24-hour sampling schedule of the observational data. Meteorological inputs for the simulation are obtained from the MM5 mesoscale model using the configuration described by Gilliam et al. (*10*). Emission inputs are grown from version 3 of EPA's 1999 National Emission Inventory (NEI) in a manner similar to the Clear Air Interstate Rule 2001 inventory (http://www.epa.gov/air/interstateairquality/). Emissions from wildfires, agricultural fires, and prescribed fires, which are significant sources of OC and EC, are allocated by state and month based on 2001 fire-activity data. The NEI does not include the major sources of non-combustion OC, such as vegetative detritus, fungal spores, and pollen grains. Additional details about the emission inputs and an operational evaluation of the 2001 CMAQ simulation results are provided by Eder and Yu (*11*).

The aerosol module in CMAQ is described by Binkowski and Roselle (*12*) and version 4.4 updates are described by Bhave et al. (*13*) and references therein. Briefly, the aerosol distribution is modeled as a superposition of three lognormal modes that correspond nominally to the ultrafine (diameter (D_p) < 0.1 μm), fine (0.1 < D_p < 2.5 μm), and coarse (D_p > 2.5 μm) particle sizes. All model results discussed in the present study are obtained by summing species concentrations over the first two modes.

In CMAQ v4.4, OC_{sec} formation occurs exclusively by absorptive partitioning of condensable oxidation products of aromatic and monoterpene compounds into a pre-existing organic-aerosol phase. Stoichiometric yields and partitioning coefficients for high- and low-yield aromatic compounds are obtained from the chamber data of Odum et al. (*14*). Yields and partitioning coefficients for cresol are estimated by Strader et al. (*15*). An emissions-based weighted-average of monoterpene yields and partitioning coefficients are constructed from the data of Griffin et al. (*16*) and the lumping approach of Bian and Bowman (*17*), using weighting factors of 0.4, 0.25, 0.15, 0.1, and 0.1, for α-pinene, β-pinene, Δ^3-carene, sabinene, and limonene, respectively. The partitioning coefficients for high- and low-yield aromatic-, cresol-, and monoterpene-oxidation products in the referenced literature are assumed to be reported at temperatures of 310, 281.5, and 313 K, respectively. These partitioning coefficients are adjusted to the ambient temperature in each model grid cell by the method of Sheehan and Bowman (*18*), assuming a 156 kJ/mol enthalpy of vaporization for all condensable organic species. The aerosol-phase concentration of each condensable species is solved iteratively, as described by Schell et al. (*19*). It is important to note that the OC_{sec} concentrations simulated using the CMAQ model are independent of the OC_{sec} concentrations obtained from eq 2. The former are modeled via the interaction between ROG and oxidant concentrations, whereas the latter are estimated from ambient measurements and the modeled ratio of two primary PM species. In this paper, the former are referred to as *mechanistic* estimates and the latter are referred to as *semi-empirical* estimates.

2.3 Observational Data. In the present study, semi-empirical estimates of OC_{pri} and OC_{sec} are made using OC and EC measurements collected in 2001 across two different monitoring networks: Interagency Monitoring of PROtected Visual Environments (IMPROVE) (http://vista.cira.colostate.edu/improve/, accessed January 2007) and South-Eastern Aerosol Research and CHaracterization (SEARCH) (http://www.atmospheric-research.com/studies/SEARCH/index.html). Among the various aerosol measurements collected during 2001, the IMPROVE and SEARCH data are selected for the present study because both networks employ a thermal-optical reflectance (TOR) protocol to distinguish OC from EC that is consistent with the protocol used to estimate most OC and EC emissions (*9*) in the NEI. Consistency in sampling protocols between the observational networks and the modeled emissions is a necessary prerequisite to applying the semi-empirical EC-tracer technique. A map of all 142 monitoring sites relevant to the current study is provided in Figure S1 (see Supporting Information). In the IMPROVE network during 2001, data were collected at 134 sites within the continental U.S. including 131 rural sites and three urban sites: Phoenix, AZ (PHOE); Washington, D.C. (WASH); and Seattle, WA (PUSO). In the SEARCH network, daily $PM_{2.5}$ OC and EC concentrations are available at eight sites including three rural sites—Yorkville, GA (YRK), Oak Grove, MS (OAK), and Centreville, AL (CTR); four urban sites—Jefferson Street in Atlanta, GA (JST), North Birmingham, AL (BHM), Gulfport, MS (GFT), and downtown Pensacola, FL (PNS); and one suburban site—Pensacola, FL (OLF). In total, 14,905 pairs of 24-hour fine-particulate OC and EC data are reported from these sites in 2001 and all of these measurements are used in the present study. The OC and EC measurement uncertainties (1σ) are assumed to be ±20% which yields ±28% uncertainty in the measured OC/EC ratios.

3. Modeled $(OC/EC)_{pri}$ Ratios

3.1 Screening for Outliers. A primary objective of this study is to evaluate mechanistically modeled OC_{sec} estimates using the semi-empirical OC_{sec} estimates. To prevent contaminating the evaluation, it is beneficial to screen out data points where the semi-empirical OC_{sec} estimates are dubious. Validity of the semi-empirical OC_{sec} estimates hinges on the accuracy of the CMAQ-modeled $(OC/EC)_{pri}$ ratios. A direct assessment of the modeled ratios cannot be conducted because the corresponding ambient ratios are not measurable. However, a myriad of methods have been developed to estimate the ambient $(OC/EC)_{pri}$ ratio from measurements and these empirically derived ratios may be used to screen the CMAQ-modeled ratios for outliers.

Each empirical method requires the identification of discrete sampling events within a study period when the ambient OC is likely to be dominated by OC_{pri}. Where intensive field data are available, such time periods have been identified using meteorological and chemical indicators including low ozone concentrations, high nitric oxide and carbon monoxide concentrations, and heavy fog or cloud cover (*3, 4, 20, 21*). In places where these indicators are not readily available, such as at the IMPROVE network sites, periods characterized by low OC_{tot}/EC ratios may be used to identify sampling events dominated by OC_{pri}. A common approach is to assume that $(OC/EC)_{pri}$ is equal to the minimum value of OC_{tot}/EC measured at a given site (*5, 22*).

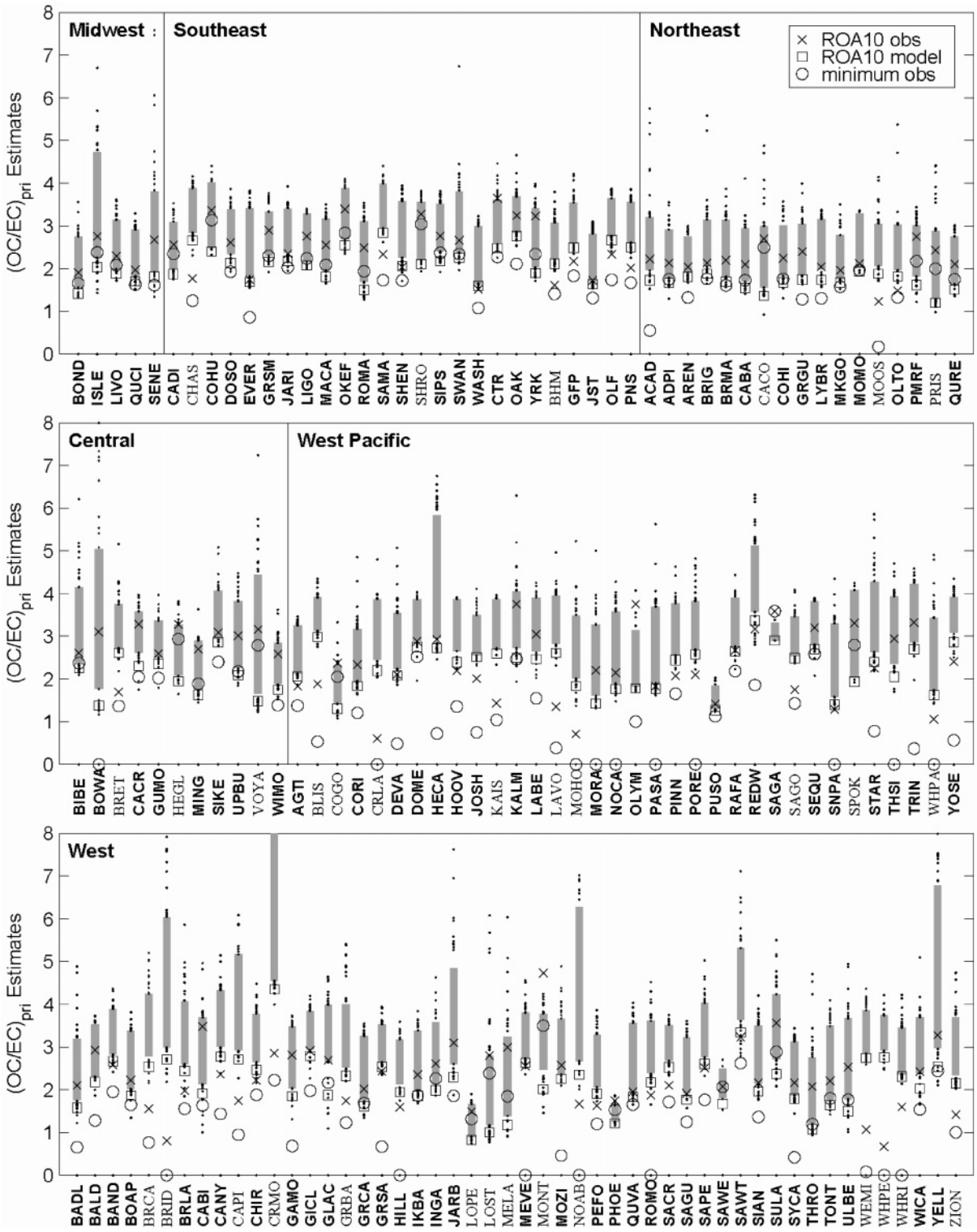

FIGURE 1. Comparison of modeled distributions and empirical estimates of $(OC/EC)_{pri}$ at each IMPROVE and SEARCH site during 2001. Gray boxes span the 10th−90th percentiles of modeled $(OC/EC)_{pri}$ ratios with dots at the outlying values. Squares correspond to ROA_{10} of the modeled $(OC/EC)_{pri}$ ratios. Bold text identifies sites where the modeled $(OC/EC)_{pri}$ ratios meet both of the acceptable criteria (see text for details).

We refer to this as the "min(OC/EC)" empirical estimate of $(OC/EC)_{pri}$. Another approach is to isolate data points whose OC_{tot}/EC ratios fall within the lowest 5 or 10 percentile of all data at that site, and apply a linear regression of OC_{tot} on EC through those data points to obtain an empirical estimate of $(OC/EC)_{pri}$ (*23*). Numerical experiments by Chu (*24*) reveal that if the non-combustion OC_{pri} is negligible, rather than applying a linear regression, a more stable estimate of $(OC/EC)_{pri}$ may be obtained from the selected data points by dividing the average OC concentration by the average EC concentration. In the present study, we calculate this ratio of averages (ROA) using all data points within the lowest 10 percentile by OC_{tot}/EC throughout the year at a given site and refer to this as the "ROA_{10}" empirical estimate of $(OC/EC)_{pri}$.

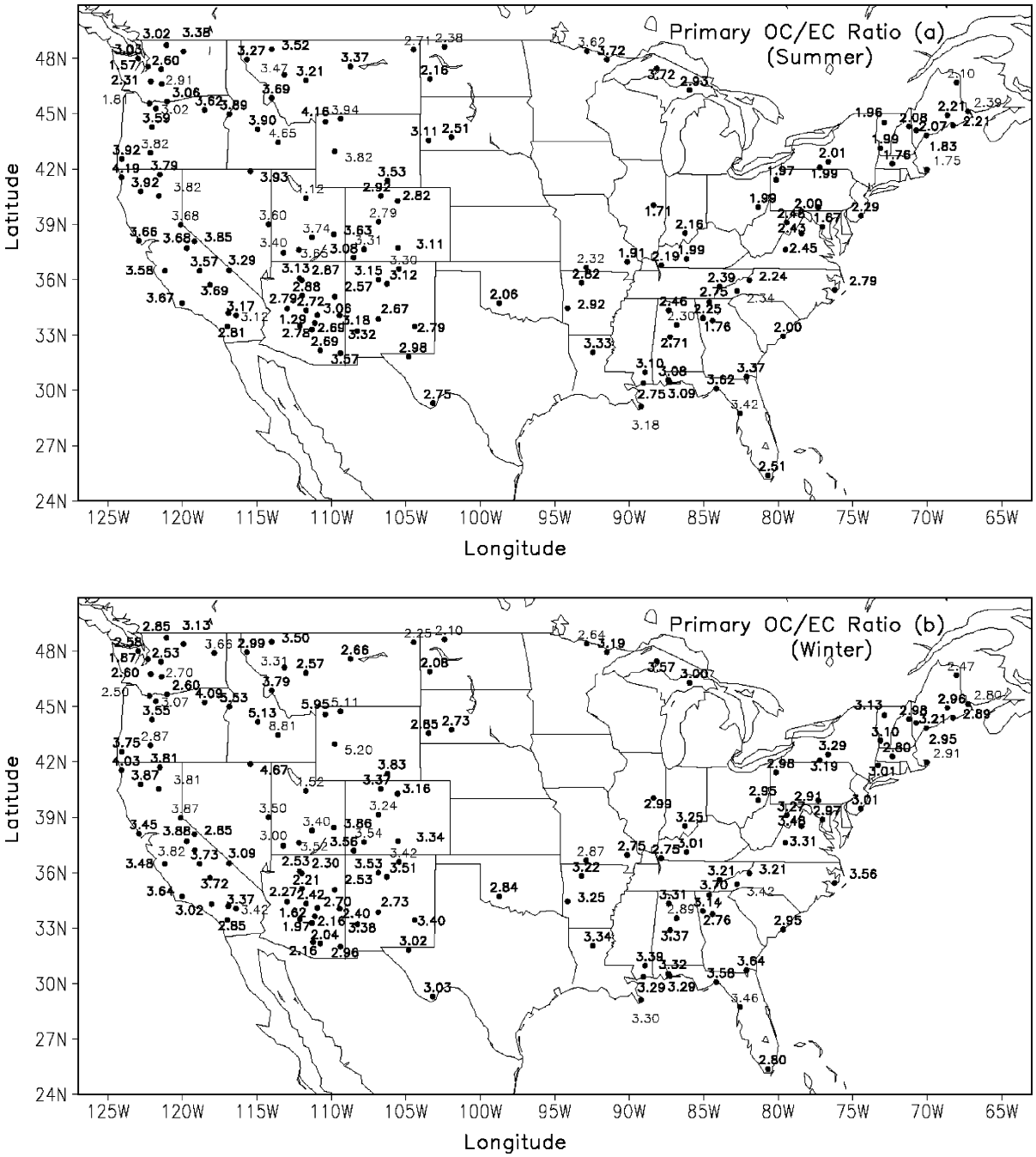

FIGURE 2. Spatial distributions of ratios of the mean modeled OC_{pri} to mean modeled EC at IMPROVE and SEARCH sites over the U.S. during (a) summer and (b) winter. Bold text identifies sites where the modeled ratios of OC_{pri} to EC are acceptable.

In Figure 1, calculations of $(OC/EC)_{pri}$ obtained from the CMAQ model and from the two empirical methods described above are compared. Whereas each empirical method yields one annual estimate of $(OC/EC)_{pri}$ at each site, the CMAQ model yields time-varying estimates of $(OC/EC)_{pri}$ throughout the year (depicted by gray boxes and dots in Figure 1). To assist in the comparison of empirical and modeled $(OC/EC)_{pri}$, the lowest 10 percentile of modeled $(OC/EC)_{pri}$ ratios at a given site are used to compute a mean(OC_{pri})/mean(EC) ratio which is referred to here as "ROA_{CMAQ}" (shown as squares in Figure 1).

Two criteria are devised to identify outliers in the modeled $(OC/EC)_{pri}$ estimates. First, sites at which ROA_{CMAQ} exceeds ROA_{10} by more than the 28% measurement uncertainty indicate that the modeled $(OC/EC)_{pri}$ ratios are too large. Note that ROA_{CMAQ} is composed entirely of primary carbon by definition whereas the empirical ROA_{10} estimate may contain some secondary carbon, so ROA_{CMAQ} should be less than ROA_{10} in the absence of measurement error. Twenty-one sites are considered outliers based on this criterion including CHAS, MOOS, and CRMO. Second, sites at which the 10th percentile value of the modeled $(OC/EC)_{pri}$ ratio falls more than 28% below min(OC/EC) indicate that the modeled ratios are too small. The 10th percentile of modeled values is chosen rather than the minimum to allow for the possibility that the min(OC/EC) observation may be contaminated with some secondary carbon. Eleven sites are classified as outliers based on this criterion including COGO, LOST, and MONT. Overall, 23 of the 32 sites designated as outliers are located in the western U.S., likely due to poor temporal and spatial allocation and highly uncertain chemical speciation of wild-fire emissions in the 2001 NEI. Future

TABLE 1. Annual, Seasonal, and Regional Medians (25th Percentile, 75th Percentile) of Semi-Empirical Estimated OC_{sec} and OC_{pri}, Percentages of OC_{sec} and OC_{pri}, and Modeled Primary OC/EC Ratios for Each Region over the United States on the Basis of Results at IMPROVE and SEARCH Sites in 2001 (N_{site} and N Are Total Numbers of Sites and Data Points, Respectively)

			semi-empirical estimates				model
	N_{site}	N	OC_{pri} (μg C m^{-3})	OC_{sec} (μg C m^{-3})	$(OC_{pri})/(OC)$ (%)	$(OC_{sec})/(OC)$ (%)	$((OC)/(EC))_{pri}$
central							
winter	11	216	0.80 (0.48, 0.87)	0.21 (0.13, 0.37)	74 (70, 80)	26 (20, 30)	3.03 (2.84, 3.24)
spring	11	308	0.99 (0.38, 1.05)	0.54 (0.40, 0.86)	55 (49, 63)	45 (37, 51)	3.21 (2.90, 3.50)
summer	11	300	0.59 (0.48, 0.86)	1.06 (0.54, 1.37)	41 (32, 43)	59 (57, 68)	2.92 (2.43, 3.29)
fall	11	313	0.78 (0.55, 1.01)	0.73 (0.43, 1.21)	52 (45, 56)	48 (44, 55)	2.72 (2.50, 2.84)
annual	11	1137	0.80 (0.46, 0.95)	0.76 (0.36, 1.03)	50 (48, 54)	50 (46, 52)	3.06 (2.67, 3.13)
midwest							
winter	5	84	0.88 (0.50, 1.06)	0.07 (0.06, 0.15)	88 (84, 95)	12 (5, 16)	3.00 (2.98, 3.33)
spring	5	123	0.89 (0.45, 0.92)	0.38 (0.32, 0.50)	65 (56, 70)	35 (30, 44)	2.39 (2.31, 2.69)
summer	5	146	0.83 (0.71, 1.01)	0.65 (0.61, 0.71)	58 (53, 60)	42 (40, 47)	2.16 (1.92, 3.13)
fall	5	155	1.08 (0.58, 1.18)	0.44 (0.41, 0.49)	70 (61, 71)	30 (29, 39)	2.54 (2.35, 2.63)
annual	5	508	0.93 (0.54, 1.07)	0.49 (0.38, 0.53)	66 (62, 67)	34 (33, 38)	2.62 (2.31, 2.79)
northeast							
winter	17	244	0.85 (0.72, 1.02)	0.12 (0.06, 0.23)	87 (79, 93)	13 (7, 21)	2.98 (2.90, 3.11)
spring	15	356	0.54 (0.41, 0.68)	0.37 (0.31, 0.50)	63 (54, 66)	37 (34, 46)	2.39 (2.33, 2.50)
summer	16	426	0.72 (0.61, 0.91)	0.83 (0.70, 0.95)	47 (41, 52)	53 (48, 59)	2.00 (1.96, 2.16)
fall	17	503	0.80 (0.57, 0.97)	0.49 (0.32, 0.58)	62 (60, 69)	38 (31, 40)	2.40 (2.27, 2.43)
annual	17	1529	0.73 (0.55, 0.98)	0.51 (0.43, 0.59)	61 (53, 66)	39 (34, 47)	2.42 (2.32, 2.54)
southeast							
winter	25	794	1.56 (1.09, 2.09)	0.29 (0.14, 0.54)	85 (74, 90)	15 (10, 26)	3.29 (3.00, 3.43)
spring	25	752	1.29 (1.01, 1.91)	0.57 (0.40, 0.79)	71 (60, 81)	29 (19, 40)	3.21 (2.88, 3.52)
summer	25	890	1.02 (0.88, 1.43)	0.93 (0.54, 1.36)	49 (41, 67)	51 (33, 59)	2.46 (2.25, 2.87)
fall	25	812	1.37 (1.05, 1.89)	0.87 (0.63, 1.02)	58 (49, 71)	42 (29, 51)	2.86 (2.66, 2.93)
annual	25	3248	1.33 (1.02, 1.75)	0.65 (0.44, 0.94)	62 (54, 75)	38 (25, 46)	2.95 (2.75, 3.25)
west							
winter	50	1216	0.31 (0.19, 0.39)	0.11 (0.05, 0.15)	76 (66, 86)	24 (14, 34)	3.08 (2.40, 3.52)
spring	49	1315	0.29 (0.24, 0.37)	0.24 (0.20, 0.37)	51 (45, 60)	49 (40, 55)	3.17 (2.58, 3.51)
summer	49	1282	0.40 (0.34, 0.49)	0.45 (0.33, 0.75)	47 (37, 53)	53 (47, 63)	3.13 (2.79, 3.54)
fall	49	1359	0.45 (0.33, 0.56)	0.24 (0.17, 0.47)	59 (50, 68)	41 (32, 50)	3.15 (2.84, 3.39)
annual	50	5172	0.38 (0.29, 0.46)	0.28 (0.21, 0.42)	55 (48, 63)	45 (37, 52)	3.11 (2.74, 3.43)
west Pacific							
winter	34	765	0.35 (0.18, 0.59)	0.08 (0.05, 0.19)	77 (64, 85)	23 (15, 36)	3.43 (2.85, 3.81)
spring	28	799	0.34 (0.26, 0.54)	0.33 (0.27, 0.43)	53 (47, 59)	47 (41, 53)	3.05 (2.38, 3.42)
summer	31	797	0.66 (0.44, 0.92)	0.49 (0.37, 0.64)	54 (47, 60)	46 (40, 53)	3.58 (3.03, 3.77)
fall	33	950	0.62 (0.43, 0.84)	0.43 (0.29, 0.68)	53 (45, 63)	47 (37, 55)	3.14 (2.40, 3.45)
annual	34	3311	0.54 (0.37, 0.76)	0.36 (0.26, 0.52)	57 (50, 60)	43 (40, 50)	3.41 (2.75, 3.63)
whole U.S.							
winter	142	3319	0.52 (0.28, 1.01)	0.13 (0.06, 0.23)	79 (70, 88)	21 (12, 30)	3.15 (2.80, 3.50)
spring	133	3653	0.42 (0.29, 0.91)	0.36 (0.23, 0.53)	56 (48, 65)	44 (35, 52)	2.99 (2.48, 3.45)
summer	137	3841	0.60 (0.41, 0.90)	0.63 (0.41, 0.94)	49 (41, 57)	51 (43, 59)	2.92 (2.32, 3.52)
fall	140	4092	0.62 (0.43, 1.02)	0.44 (0.27, 0.75)	58 (50, 68)	42 (32, 50)	2.86 (2.43, 3.22)
annual	142	14905	0.54 (0.38, 0.97)	0.42 (0.27, 0.59)	57 (51, 64)	43 (36, 49)	2.99 (2.58, 3.40)

applications of the semi-empirical technique over the western U.S. should benefit greatly from recent efforts to improve wild-fire emission estimates in that region. In the eastern U.S., only 9 out of 58 sites are identified as outliers. Four of these are located along the coastline (CHAS, CACO, MOOS, and BRET) and one is amidst complex terrain (SHRO), where ambient concentrations tend to be poorly represented in regional-scale Eulerian models (*11*). In total, 110 of 142 sites (77.5%) are deemed acceptable after screening for outliers. These sites are identified with boldface type in Figures 1−3.

It is worthwhile to comment on the advantages of using modeled ratios in lieu of empirically derived ratios to estimate OC_{pri} and OC_{sec} concentrations. First, most empirical methods yield only a single value of $(OC/EC)_{pri}$ for an entire study period. Measurements collected by other investigators (*25, 26*) provide strong evidence that controverts the use of time-invariant $(OC/EC)_{pri}$ ratios for OC_{sec} estimation. The broad temporal distributions of modeled ratios at many sites shown in Figure 1 provide additional evidence to this end. Second, the results displayed in Figure S2 (see Supporting Information) indicate that the semi-empirical estimates of OC_{sec} after screening for outliers are in reasonable agreement with the empirical estimates, and may be superior to empirical estimates during the winter season. In spite of these advantages, it is important to emphasize that the semi-empirical OC_{sec} estimates, like all empirical estimates, have limitations and there is no standard or perfect method of OC_{sec} estimation.

3.2 Seasonal and Regional Analyses over the United States. Figure 2 presents the modeled $(OC/EC)_{pri}$ ratios at the IMPROVE and SEARCH sites during summer and winter; sites with acceptable modeled ratios are shown in bold. As discussed previously, the CMAQ modeled $(OC/EC)_{pri}$ ratios are acceptable at 84% of sites in the eastern U.S. (49 out of 58) and 73% in the western U.S. (61 out of 84). In the subsequent discussion, we will only focus on those sites where the modeled ratios are deemed acceptable. The summer mean $(OC/EC)_{pri}$ ratios can vary substantially from 1.12 at Lone Peak Wilderness, UT (LOPE) to 4.16 at Yellowstone National Park, WY (YELL), whereas the winter mean $(OC/EC)_{pri}$ ratios vary from 1.52 at the LOPE site to 5.95 at the YELL site. A comparison of both panels in Figure 2 reveals that the winter mean $(OC/EC)_{pri}$ ratios at most sites are generally higher than the corresponding summer values over the eastern regions, while the differences in winter and summer mean $(OC/EC)_{pri}$ ratios are relatively small across

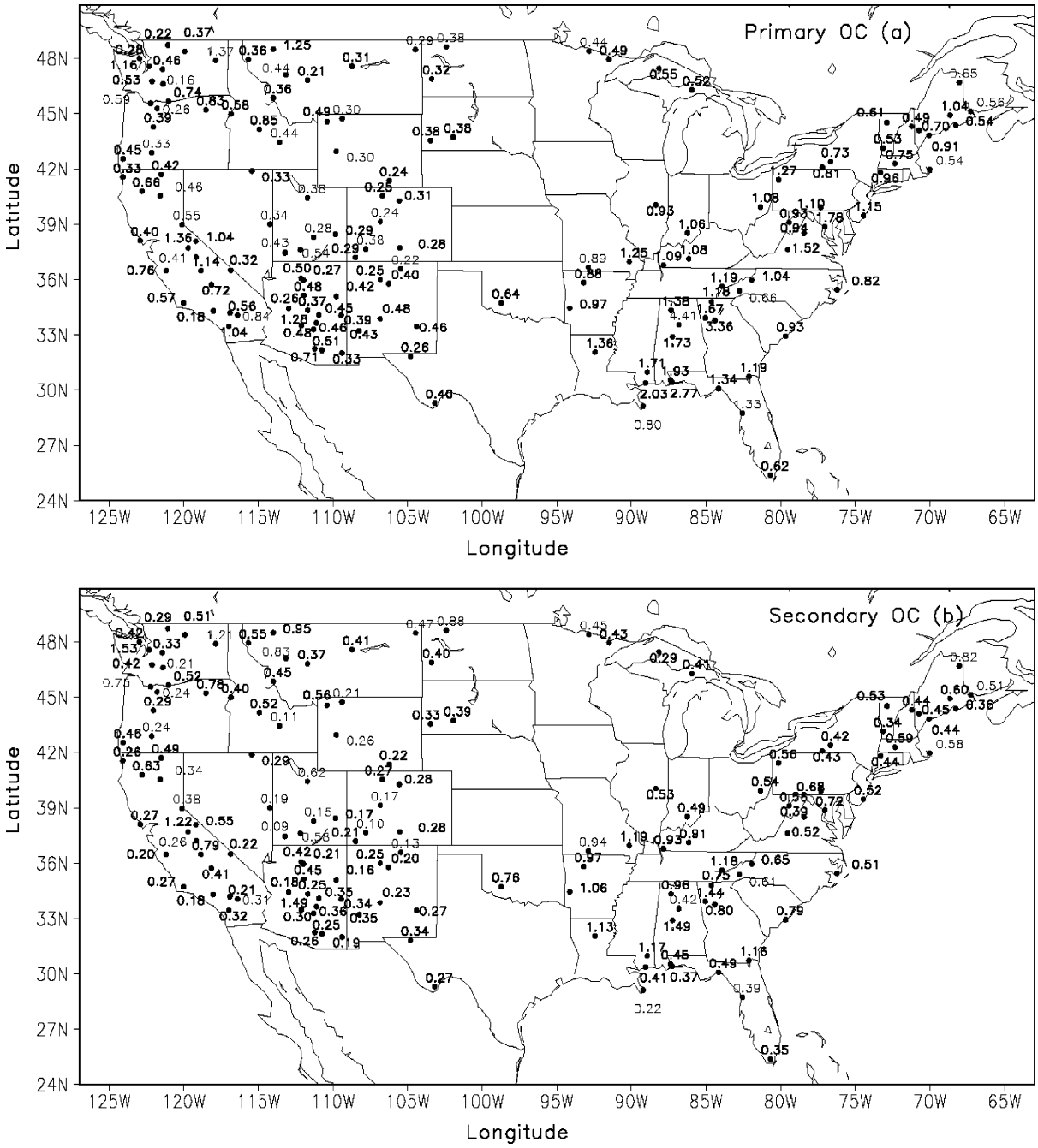

FIGURE 3. Spatial distributions of annual mean semi-empirical estimates of (a) OC_{pri} and (b) OC_{sec} concentrations (μg C m^{-3}) at each site over the United States. Bold text identifies sites where the modeled ratios of OC_{pri} to EC are acceptable.

the western regions. Table 1 also shows that over the northeast, southeast, and midwest, the winter median $(OC/EC)_{pri}$ ratios are higher than those from all other seasons (2.00−2.95). This is due to the fact that residential wood combustion and natural gas combustion increase during winter and these emission sources have high OC/EC ratios (see Table 1s). In the central region, the median $(OC/EC)_{pri}$ ratio peaks during the spring because it is dominated by agricultural burning activities which also yield high OC/EC ratios. The generally higher $(OC/EC)_{pri}$ ratios in the western regions relative to the east are influenced by widespread wild and prescribed fire activities (*27*) and lower vehicle exhaust contributions year round. Ames et al. (*28*) estimated that wildland fire smoke plumes can contribute from 10 to 70% of measured OC annually over the continental United States. Chow et al. (*29*) showed that the $(OC/EC)_{pri}$ ratios from motor vehicles measured in a California tunnel were typically about 0.7 but those in Colorado hardwood smoke were in the 7.9−8.6 range. For residential wood combustion, McDonald et al. (*30*) also found high $(OC/EC)_{pri}$ ratios (3.9−9.0) for a variety of wood types used in residential wood combustion. Kirchstetter et al. (*31*) also found that $(OC/EC)_{pri}$ ratios of automotive emissions in California from diesel and gasoline engines are 0.5 ± 0.4 and 0.9 ± 0.4, respectively. Obviously, the mean $(OC/EC)_{pri}$ ratios at each site represent a combined result from multiple sources.

4. Results and Discussion

4.1 Seasonal and Regional Analyses of Semi-Empirical Estimates of OC_{pri} and OC_{sec}. As shown in Table 1, the nationwide median OC_{sec} concentrations estimated by the semi-empirical method are 0.13, 0.36, 0.63, 0.44, and 0.42 μg C m^{-3} for winter, spring, summer, fall, and year, respectively, corresponding to 21, 44, 51, 42, and 43% contributions to

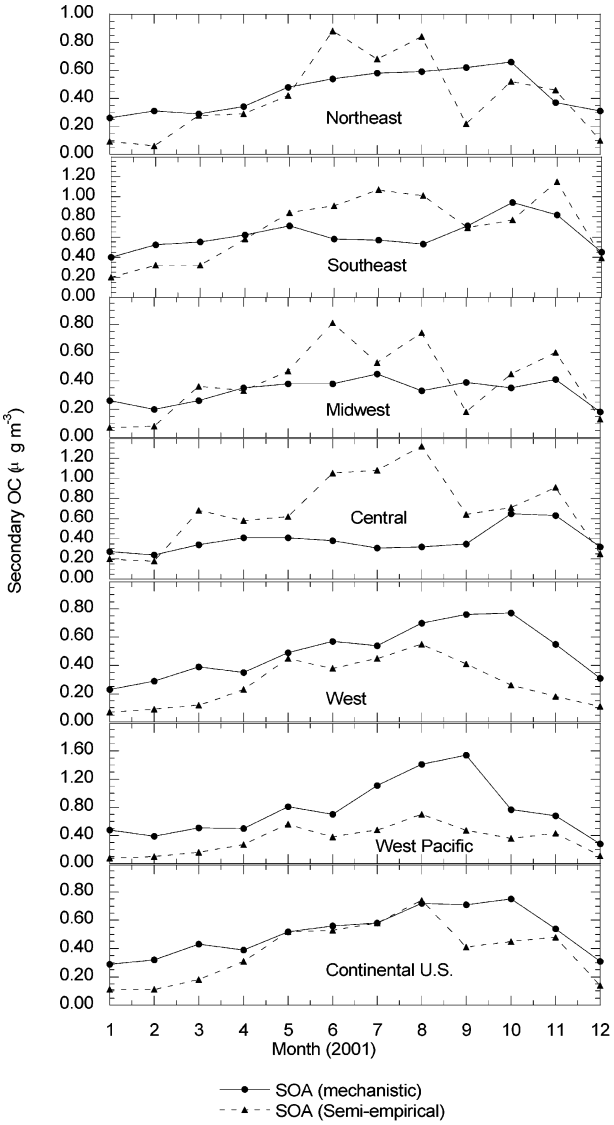

FIGURE 4. Time series of monthly medians of semi-empirical and mechanistic estimates of OC_{sec} in each region excluding the sites identified as outliers in Section 3.1.

OC, respectively. Similar trends are also noted for the various subregions. The high summer OC_{sec} is consistent with photochemical activity in summer that would lead to OC_{sec} formation. On a regional basis, the southeastern region has the highest concentrations of both OC_{pri} and OC_{sec} concentrations (annual median OC_{pri}, 1.33 μg C m^{-3}; and OC_{sec}, 0.65 μg C m^{-3}) in all seasons except summer, when the central region has the highest median OC_{sec} of 1.06 μg C m^{-3}. As expected, OC_{pri} accounts for a large fraction of OC in all regions ($\geq$74%) during winter.

Figure 3 presents the estimated annual average OC_{pri} and OC_{sec} concentrations using the semi-empirical method. Relatively higher OC_{pri} and OC_{sec} concentrations are noted in the east compared to other parts of the United States. The annual mean OC_{sec} concentrations vary greatly from 0.25 μg C m^{-3} at Ike's Backbone, AZ (IKBA) to 1.49 μg C m^{-3} at the CTR site, AL, while the annual mean OC_{pri} concentrations range from 0.21 μg C m^{-3} at Gates of the Mountains, MT (GAMO) to 3.36 μg C m^{-3} at the JST site. The annual mean OC_{pri} concentration exceeds OC_{sec} at 91 out of 110 acceptable sites across the United States.

4.2 Testing Mechanistic Model Calculations of OC_{sec}. To assess the model's ability to simulate the distributions of OC_{sec} (produced from the oxidation of anthropogenic aromatic compounds and biogenic terpenes), we compare the modeled OC_{sec} values with the semi-empirical OC_{sec} estimates. The mechanistic model predictions of OC_{sec} may be regarded as independent of the semi-empirical OC_{sec} estimates as discussed in Section 2.2. The sites identified as outliers in Section 3.1 are omitted from this comparison. Figure 4 shows time-series comparisons of the median monthly OC_{sec} concentrations obtained from the model and semi-empirical methods for each region. As can be seen, the model reproduces the semi-empirical estimates for each region and each month reasonably well. For example, the model reproduces the monthly medians of the semi-empirical estimated OC_{sec} well over the northeast, southeast, midwest, and central regions in January−May and October−December when the OC_{sec} concentrations are relatively low. The model overpredicts OC_{sec} concentrations in the northeast and midwest regions during September. In the summer months (June, July, and August) in the central and eastern U.S., the modeled regional monthly medians are consistently lower than the semi-empirical estimates. The underprediction is especially large in the southeast and central regions. The underpredictions of both OC_{sec} and OC_{pri} result in the underprediction of the modeled OC (not shown) during the summer season over these regions. Factors contributing to this underprediction include: (1) missing sources of OC_{pri} in the summer emission inventory (32), and (2) possible underestimation of OC_{sec} formation such as sources from the oxidation of isoprene and sesquiterpenes (*33, 34*) that are not included in the CMAQ. Morris et al. (*33*) found that including the SOA formation from sesquiterpenes and isoprene can improve the CMAQ model performance for OC. The modeled regional monthly median OC_{sec} concentrations are consistently higher than the semi-empirical estimates over the western and west Pacific regions. The ovepreduction is especially large in late summer over the west Pacific region, possibly due to overestimations of monoterpene emissions in the model (*33*). This evaluation reveals that summertime model concentrations of OC_{sec} fall substantially below the semi-empirical estimates over the southeast and greatly exceed the semi-empirical estimates in the west. It is important to improve mechanistic estimates of OC_{sec} during the summer season, when it makes the largest contribution to fine particulate matter concentrations.

Acknowledgments

We thank S. T. Rao, Venkatesh Rao, and Shao-Hang Chu for valuable comments during the preparation of this manuscript. This work has been subjected to U.S. Environmental Protection Agency peer review and approved for publication. The research presented here was performed under the Memorandum of Understanding between the U.S. Environmental Protection Agency (EPA) and the U.S. Department of Commerce's National Oceanic and Atmospheric Administration (NOAA) and under agreement number DW13921548. This work constitutes a contribution to the NOAA Air Quality Program. Although it has been reviewed by EPA and NOAA and approved for publication, it does not necessarily reflect their policies or views.

Supporting Information Available

Map of 142 monitoring sites, comparison of semi-empirical and empirical OC_{sec} estimates, and top 10 profiles for 2001 $PM_{2.5}$ OC and EC emissions. This material is available free of charge via the Internet at http://pubs.acs.org.

Literature Cited

(1) U.S. EPA. *National Air Quality and Emissions Trends Report*; EPA 454/R-03-005; Washington, DC, 2003.

(2) Turpin, B. J.; Saxena, P.; Andrews, E. Measuring and simulating particulate organics in the atmosphere: problems and prospects. *Atmos. Environ.* **2000**, *34*, 2983−3013.

(3) Turpin, B. J.; Huntzicker, J. J. Identification of secondary organic aerosol episodes and quantitation of primary and secondary organic aerosol concentrations during SCAQS. *Atmos. Environ.* **1995**, *29*, 3527−3544.
(4) Cabada, J. C.; Takahama, S.; Khlystov, A.; Pandis, S. N.; Rees, S.; Davidson, C. I.; Robinson, A. L. Mass size distributions and size resolved chemical composition of fine particulate matter at the Pittsburgh Supersite. *Atmos. Environ.* **2004**, *38*, 3127−3141.
(5) Castro, L. M.; Pio, C. A.; Harrison, R. M.; Smith, D. J. T. Carbonaceous aerosol in urban and rural European atmospheres: estimate of secondary organic carbon concentrations. *Atmos. Environ.* **1999**, *33*, 2771−2781.
(6) Schauer, J. J.; Rogge, W. F.; Hildemann, L. M.; Mazurek, M. A.; Cass, G. R.; Simoneit, B. R. T. Source apportionment of airborne particulate matter using organic compounds as tracers. *Atmos. Environ.* **1996**, *22*, 3837−3855.
(7) Zheng, M.; Cass, G. R.; Schauer, J. J.; Edgerton, E. S. Source apportionment of PM2.5 in the southeastern United States using solvent-extractable organic compounds as tracers. *Environ. Sci. Technol.* **2002**, *36*, 2361−2371.
(8) Sheesley, R. J.; Schauer, J. J.; Bean, E.; Kenski, D. Trends in secondary organic aerosol at a remote site in Michigan's Upper Peninsula. *Environ. Sci. Technol.* **2004**, *38* (24), 6491−6500.
(9) Yu, S. C.; Dennis, R. L.; Bhave, P. V.; Eder, B. K. Primary and secondary organic aerosols over the United States: estimates on the basis of observed organic carbon (OC) and elemental carbon (EC), and air quality modeled primary OC/EC ratios. *Atmos. Environ.* **2004**, *38*, 5257−5268.
(10) Gilliam, R. C.; Hogrefe, C.; Rao, S. T. New methods for evaluating meteorological models used in air quality applications. *Atmos. Environ.* **2006**, *40*, 5073−5086.
(11) Eder, B.; Yu, S. C. A performance evaluation of the 2004 release of Models-3 CMAQ. *Atmos. Environ.* **2006**, *40*, 4811−4824.
(12) Binkowski, F. S.; Roselle, S. J. Models-3 Community Multi-scale Air Quality (CMAQ) model aerosol component: 1. Model description. *J. Geophys. Res.* **2003**, 108 (D6), 4183; doi: 10.1029/2001JD001409.
(13) Bhave, P. V.; Roselle, S. J.; Binkowski, F. S.; Nolte, C. G.; Yu, S. C.; Gipson, G. L.; Schere, K. L. CMAQ aerosol module development: Recent enhancements and future plans. Presentation at the 2004 Models-3/CMAQ Conference, October 18−20, 2004, Chapel Hill, NC, 2004.
(14) Odum, J. R.; Jungkamp, T. P. W.; Griffin, R. J.; Flagan, R. C.; Seinfeld, J. H. The atmospheric aerosol-forming potential of whole gasoline vapor. *Science* **1997**, *276*, 96−99.
(15) Strader, R.; Lurmann, F.; Pandis, S. N. Evaluation of secondary organic aerosol formation in winter. *Atmos. Environ.* **1999**, *33*, 4849−4863.
(16) Griffin, R. J.; Cocker, D. R., III; Flagan, R. C.; Seinfeld, J. H. Organic aerosol formation from the oxidation of biogenic hydrocarbons. *J. Geophys. Res.* **1999**, *104*, 3555−3567.
(17) Bian, F.; Bowman, F. M. Theoretical method for lumping multicomponent secondary organic aerosol mixtures. *Environ. Sci. Technol.* **2002**, *36* (11), 2491−2497.
(18) Sheehan, P. E.; Bowman, F. M. Estimated effects of temperature on secondary organic aerosol concentrations. *Environ. Sci. Technol.* **2001**, *35* (11), 2129−2135.
(19) Schell, B.; Ackermann, I. J.; Hass, H.; Binkowski, F. S.; Ebel, A. Modeling the formation of secondary organic aerosol within a comprehensive air quality model system. *J. Geophys. Res.* **2001**, *106*, 28275−28293.
(20) Saylor, R. D.; Edgerton, E. S.; Hartsell, B. E. Linear regression techniques for use in the EC tracer method of secondary organic aerosol estimation. *Atmos. Environ.* **2006**, *40*, 7546−7556.
(21) Russell, M.; Allen, D. T. Seasonal and spatial trends in primary and secondary organic carbon concentrations in southeast Texas. *Atmos. Environ.* **2004**, *38*, 3225−3239.
(22) Cao, J. J.; Lee, S. C.; Ho, K. F.; Zhang, X. Y.; Zou, S. C.; Fung, K.; Chow, J. C.; Watson, J. G. Characteristics of carbonaceous aerosol in Pearl River Delta Region, China during 2001 winter period. *Atmos. Environ.* **2003**, *37*, 1451−1460.
(23) Lim, H.-J.; Turpin, B. J. Origins of primary and secondary organic aerosol in Atlanta: Results of time-resolved measurements during the Atlanta Supersite Experiment. *Environ. Sci. Technol.* **2002**, *36* (21), 4489−4496.
(24) Chu, S.-H. Stable estimate of primary OC/EC ratios in the EC tracer method. *Atmos. Environ.* **2005**, *39*, 1383−1392.
(25) Bae, M.-S.; Schauer, J. J.; DeMinter, J. T.; Turner, J. R.; Smith, D.; Cary, R. A. Validation of a semi-continuous instrument for elemental carbon and organic carbon using a thermal-optical method. *Atmos. Environ.* **2004**, *38*, 2885−2893.
(26) Harley, R. A.; Marr, L. C.; Lehner, J. K.; Giddings, S. H. Changes in motor vehicle emissions on diurnal to decadal time scales and effects on atmospheric composition. *Environ. Sci. Technol.* **2005**, *39* (14), 5356−5362.
(27) Roy, B.; Pouliot, G. A.; Gilliland, A.; Pierce, T.; Howard, S.; Bhave, P. V.; Benjey, W. Refining fire emissions for air quality modeling with remotely sensed fire counts: A wildfire case study. *Atmos. Environ.* **2006**, *41*, 655−665.
(28) Ames, R. B.; Fox, D. G.; Malm, W. C.; Schichtel, B. A. *Preliminary apportionments of carbonaceous aerosols to wild fire smoke using observations from the IMPROVE network*; Regional haze paper #76; AWMA: Asheville, NC, 2004.
(29) Chow, J. C.; Watson, J. G.; Crow, D.; Lowenthal, D. H.; Merrifield, T. Comparison of IMPROVE and NIOSH carbon measurements. *Aerosol Sci. Technol.* **2001**, *34*, 23−34.
(30) McDonald, R. D.; Zielinska, B.; Fujita, E. M.; Sagebiel, J. C.; Chow, J. C.; Watson, J. G. Fine particle and gaseous emission rates from residential wood combustion. *Environ. Sci. Technol.* **2000**, *34* (11), 2080−2091.
(31) Kirchstetter, T. W., et al. Characterization of particle and gas phase pollutant emissions from heavy- and light-duty vehicles in a California roadway tunnel. *Eos Trans. AGU* **2004**, *85* (47), Fall Meeting. Suppl., Abstract A11A-0021.
(32) Bhave, P. V.; Pouliot, G. A.; Zheng, M. Diagnostic model evaluation for carbonaceous $PM_{2.5}$ using organic markers measured in the southeastern U. S. *Environ. Sci. Technol.* **2007**, *41* (5), 1577−1583.
(33) Morris, R. E.; Koo, B.; Guenther, A.; Yarwood, G.; McNally, D.; Tesche, T. W.; Tonneseon, G.; Boylan, J.; Brewer, P. Model sensitivity evaluation for organic carbon using two multi-pollutant air quality models that simulate regional haze in the southeastern United States. *Atmos. Environ.* **2006**, *40*, 4960−4972.
(34) Edney, E. O.; Kleindienst, T. E.; Jaoui, M.; Lewandowski, M.; Offenberg, J. H.; Wang, W.; Claeys, M. Formation of 2-methyl tetrols and 2-methylglyceric acid in secondary organic aerosol from laboratory irradiated isoprene/NO_x/SO_2/air mixtures and their detection in ambient $PM_{2.5}$ samples collected in the eastern United States. *Atmos. Environ.* **2005**, *39*, 5281−5289.

Received for review June 28, 2006. Revised manuscript received February 6, 2007. Accepted April 5, 2007.

ES061535G